

NUMERICAL METHODS FOR UNSATURATED FLOW WITH DYNAMIC CAPILLARY PRESSURE IN HETEROGENEOUS POROUS MEDIA

MALGORZATA PESZYŃSKA AND SON-YOUNG YI

Abstract. Traditional unsaturated flow models use a capillary pressure-saturation relationship determined under static conditions. Recently it was proposed to extend this relationship to include dynamic effects and in particular flow rates. In this paper, we consider numerical modeling of unsaturated flow models incorporating dynamic capillary pressure terms. The resulting model equations are of nonlinear degenerate pseudo-parabolic type with or without convection terms, and follow either Richards' equation or the full two-phase flow model. We systematically study the difficulties associated with numerical approximation of such equations using two classes of methods, a cell-centered finite difference method (FD) and a locally conservative Eulerian-Lagrangian method (LCELM) based on the finite difference method. We discuss convergence of the methods and extensions to heterogeneous porous media with different rock types. In convection-dominated cases and for large dynamic effects instabilities may arise for some of the methods while those are absent in other cases.

Key Words. unsaturated flow, Richards' equation, two-phase flow model, dynamic capillary pressure, pseudo-parabolic equation, finite difference method, locally conservative Eulerian-Lagrangian method, implicit time-stepping

1. Introduction

The main interest of this paper is in numerical algorithms for unsaturated flow in highly heterogeneous media and in particular handling dynamic capillary pressure.

Unsaturated preferential flow in porous media is a physical phenomenon occurring in heterogeneous soils and bedrock and is related to the presence of special features of the medium such as cracks, fissures, and macropores. Such heterogeneities are represented in partial differential equation (PDE) models of the flow by a variation of nonlinear *rock properties* of the medium with position, called the *rock type* dependence. Here we are concerned mainly with the capillary pressure function; that is, the pressure-saturation relationship $S \mapsto P_c(S)$ which, when this property is rock type dependent, it reads $S \mapsto P_c(\mathbf{x}, S)$, where \mathbf{x} denotes position. It is standard practice to include rock type dependence in a reservoir simulator [47]; however, there are few associated mathematical and numerical analyses except [18, 33] and those for multiscale heterogeneities developed in [28, 19, 16, 17].

Additional phenomena occurring in preferential flow such as nonequilibrium effects, hysteresis, and/or large flow velocities have been recently discussed by experimental and theoretical soil physicists. In particular, it has been observed and reconfirmed recently, see [66] and references therein, that rock properties measured

1991 *Mathematics Subject Classification.* AMS(MOS) subject classifications. 35K65, 35K70, 65M06, 76S05.

in a laboratory in equilibrium conditions bear little resemblance to those observed in experiments in case of large fluxes (velocities); it has been in fact postulated that the data collected especially for the capillary pressure has a non-unique character when considered over a range of nonequilibrium conditions. This suggests existence of a hidden variable as pointed out in [41] and can be explained in terms of the imbibition (increasing S) and drainage (decreasing S) hysteresis. Another recently proposed class of model modifications has been the use of *dynamic capillary pressure* [42, 68, 67, 66, 12, 11] which accounts for the dynamic flow rates via $S \mapsto P_c(\mathbf{x}, S, \frac{dS}{dt})$. Some authors believe that dynamic capillary pressure terms could explain instabilities in gravity-driven flow and in particular the phenomena of fingering [51]. Finally, there is evidence that in the presence of strong heterogeneities the conditions at the interface of different rock types should reflect non-equilibrium [55, 19].

Our interest is in numerical modeling of preferential flow in porous media which may occur at more than one scale through macropores or due to small or large inhomogeneities as well as in rock fractures, gravel filled excavated areas etc. Therefore, it is necessary for us to explore the numerical algorithms for dynamic capillary pressure and multiple rock types.

From a theoretical PDE point of view, Richards' model of unsaturated flow is a nonlinear degenerate parabolic equation in the unknown water saturation S ; its character depends on the nonlinear diffusion parameter $\mathbf{D}(S)$ which may become degenerate (zero or very large) for some values of S . In addition, if the flow has vertical components, then the associated nontrivial convective term competes with the nonlinear degenerate diffusion. Depending on the rock type and initial and boundary conditions of the flow, the solutions may be smooth or may exhibit sharp fronts [4, 5, 6].

The presence of dynamic capillary pressure terms changes the type of original nonlinear degenerate parabolic PDEs to *pseudo-parabolic*, with the additional nonlinear degenerate term being proportional to a coefficient τ , see development in Section 2.3. Available existence, uniqueness, and regularity theory for pseudo-parabolic equations [58, 60, 61] predicts that the additional pseudo-parabolic term decreases the smoothing property characteristic to parabolic problems (if at all present) to a factor involving $e^{-\tau}$. In addition it is known that there is in general no maximum principle for pseudo-parabolic equations such as one expected of solutions to parabolic equations. Finally, we note that the available theory may or may not include cases with dominating and degenerate convection; assumptions need to be verified on a case by case basis.

Numerical methods for Richards' equation include practical implementations of finite difference [69], finite elements [69, 40, 44, 54], finite volumes [1] and characteristic-based methods [7]; we do not attempt to give a comprehensive review here. Typically, convergence results are formulated for either transformed variables or for cases away from degeneracy, or for regularized problem. See, e.g., [9, 36] for results and references using Kirchoff transformation, and [33] for those using similarity solutions. Numerical methods for Richards' equation in physical variables have been used in hydrology [20] but have not been analyzed outside smooth regimes where standard convergence rates apply. Furthermore, there exist a plethora of methods applicable to two-phase flow formulation of unsaturated flow, see [25, 43, 22, 23, 21]; however, similarly to the case of Richards' equation, those results have been formulated for transformed variables or for smooth regime(s). Finally, comparison of two-phase flow versus Richards' formulations have been studied

in [62, 44, 64]; these point out that in some regimes the use of Richards' equation leads to loss of information.

On the other hand, there exist discretizations and associated analysis for (single) pseudo-parabolic equations given in [35, 10, 38, 39, 37] but these theoretical convergence results do not indicate any difficulties associated with large convective (advective) terms. Possibly such cases are ruled out by assumptions on the smoothness of the analytical solution necessary to obtain convergence results.

However, the reported numerical simulation results point out difficulties in incorporating dynamic capillary pressure and stipulate that the problems are properties of the numerical method [42] or of the PDE's themselves [51]. Most of these results focus on the modeling aspects of dynamic capillary pressure and on the identification of the coefficient τ ; τ appears not to be constant especially in heterogeneous media [42, 49]. We also note that the combination of dynamic capillary pressure with *play-type hysteresis*, for a nonlinear non-degenerate case of horizontal flow, is discussed in [13]. Among these results, [42] and [49] appear to use traditional discretizations of Richards' and two-phase formulations, respectively. The work [51] seeks similarity and traveling wave solutions. The approach in [13] leads to solving a time-lagged coupled system of two equations, the first of which is elliptic and is solved for pressure, while the second is an ODE for saturation. In the quoted results we did not find detailed formulation of numerical algorithm, or convergence analysis/studies.

As a point of departure for this paper, we consider numerical methods which apply to nontransformed, nonregularized model(s) of unsaturated preferential flow in porous media with strong heterogeneities and with locally large fluxes. We are interested in both Richards' and two-phase formulations. We systematically study the difficulties associated with the numerical approximation of dynamic capillary pressure terms. Since the reported numerical simulation results on dynamic capillary pressure using traditional methods appear to exhibit instabilities, our approach is to carefully formulate different variants, study their convergence and finally detect the presence of instabilities if any. In an effort to be inclusive, we include a large set of prototypes (variants) of the traditional methods from the finite difference (FD) family to determine whether a particular detail of discretization may be the factor that triggers the instabilities. The variants therefore include various ways of averaging, implicit or semi-implicit solutions, and different choices of primary unknowns. In addition to the FD family, we formulate and investigate a different class of models which enables a locally conservative handling of convection terms (LCELM family) combined with FD treatment of nonlinear diffusion. All these discretizations are proposed for Richards' equation.

Moreover, we discuss a numerical formulation for the full two-phase flow model which is more general than Richards' equation; we allow for different rock types and dynamic capillary pressure and compare solutions to those for Richards' equation. Our formulations and discussion are supported by convergence studies and the numerical simulation results are illustrated. Finally, we consider a representative cell of a multiscale heterogeneous medium; discussion of a full simulation of preferential flow with dynamic effects is outside the scope here; to our knowledge such a study has not been undertaken.

Below in Section 2 we discuss the physical models, in Section 3 we formulate the numerical methods, and in Section 4 we present convergence studies and simulation results. The paper closes with Conclusions and Acknowledgements.

2. Physical model

Consider a porous medium: an open bounded domain $\Omega \subset \mathbb{R}^d$, with $d = 1, 2, 3$, characterized by physical properties of porosity $\phi = \phi(\mathbf{x}) > 0$ and (absolute) permeability $\mathbf{K} = \mathbf{K}(\mathbf{x}) \in \mathbb{R}^{d \times d}$, the latter in general heterogeneous and anisotropic. Here we assume as it is usually done that \mathbf{K} is uniformly positive definite. In addition, let \mathbf{K} be diagonal, i.e. its variability is aligned with coordinate axis.

Furthermore, let us be given for convenience, in the given coordinate system, the value of depth of the porous medium $D(\mathbf{x})$ under the earth's surface. We set

- (1) $i) D(\mathbf{x}) \equiv 0$: horizontal flow case,
- (2) $ii) D(\mathbf{x}) = x$: vertical infiltration problem.

The governing equations for the flow of two immiscible fluids in this porous medium are given by the full two-phase flow model (3)–(4) or by the Richards' equation model to be defined below (18) which is a simplified version of the two-phase model. The models are standard [52, 24, 43, 50]. We briefly recall the formulation(s) for completeness.

The two phases are denoted by subscripts α whereby $\alpha = w$ refers to water (wetting phase) and $\alpha = n$ refers to the other (nonwetting) phase which may be air or a hydrocarbon phase/component. The fluids have densities ρ_w, ρ_n and viscosities μ_w, μ_n , respectively. For simplicity, if no subscript is used, this denotes by default the wetting phase, i.e.. $\mu \equiv \mu_w, \rho \equiv \rho_w$ etc. The flow is described by the equations

$$\begin{aligned}
 (3) \quad & \phi \frac{\partial S}{\partial t} - \nabla \cdot \left(\frac{1}{\mu} \mathbf{K} k_w(\mathbf{x}, S) (\nabla P - \rho G \nabla D) \right) = 0, \quad \mathbf{x} \in \Omega, t > 0, \\
 (4) \quad & \phi \frac{\partial S_n}{\partial t} - \nabla \cdot \left(\frac{1}{\mu_n} \mathbf{K} k_n(\mathbf{x}, S) (\nabla P_n - \rho_n G \nabla D) \right) = 0, \quad \mathbf{x} \in \Omega, t > 0, \\
 (5) \quad & P_n - P = P_c(\mathbf{x}, S).
 \end{aligned}$$

In this model we have incorporated conservation of mass and multiphase extension of Darcy's law for immiscible two-phase fluids, which for each phase α , in the absence of external sources, read, respectively, $\phi \frac{\partial \rho_\alpha S_\alpha}{\partial t} + \nabla \cdot (\rho_\alpha \mathbf{u}_\alpha) = 0$ and $\mathbf{u}_\alpha = -\frac{\mathbf{K} k_\alpha}{\mu_\alpha} (\nabla P_\alpha - \rho_\alpha G \nabla D)$. The incompressibility assumption allows for the elimination of the constant densities from the formulation everywhere except in the gravity terms $\rho_\alpha G \nabla D$.

The unknowns of the system are the saturations S, S_n related by

$$(6) \quad S + S_n \equiv 1,$$

and the pressures P, P_n . These unknowns are related to each other by (5), or by its extension(s) to be discussed.

Here the rock-fluid properties are the capillary pressure relationship (5) and relative permeabilities k_w, k_n which are functions of the wetting phase saturation S and as such take values in $[0, 1]$ and are, respectively, nondecreasing and nonincreasing. Their dependence on \mathbf{x} reflects heterogeneity of rocks and in particular the fact that in a domain composed of different rock types, for example, containing coarse and fine sand, the properties k_w, k_n, P_c will be given by different functional relationships, see Figure 1.

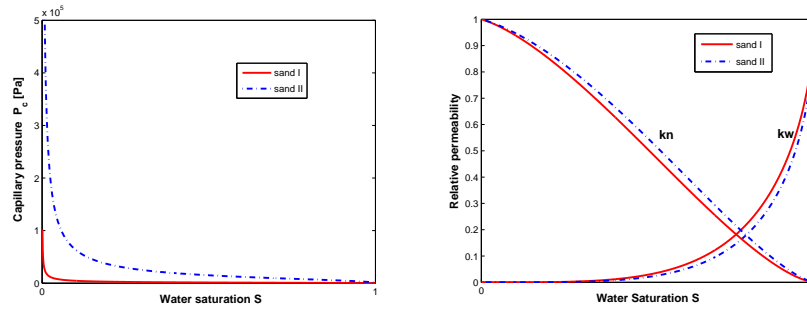


FIGURE 1. Capillary pressure (left) and relative permeabilities (right) for two rock types: sand I (coarse), and sand II (fine). Here we use van Genuchten model with data as in Table 4.1.

In numerical examples in this paper we use the so-called van-Genuchten–Mualem model in which

$$(7) \quad P_c(S) = \frac{1}{\alpha} (S^{-\frac{1}{m}} - 1)^{\frac{1}{n}},$$

$$(8) \quad k_w(S) = S^\epsilon \left[1 - \left(1 - S^{\frac{1}{m}} \right)^m \right]^2,$$

(9)

$$(10) \quad k_n(S) = (1 - S)^\gamma \left[1 - S^{\frac{1}{m}} \right]^{2m}.$$

Generally, $\epsilon = \frac{1}{2}$, $\gamma = \frac{1}{3}$ and $m = 1 - \frac{1}{n}$, and α, n are given from experiments. Rock type dependent k_w, k_n and P_c can be determined by $\alpha(\mathbf{x})$ and $n(\mathbf{x})$.

For the case when k_w, k_n, P_c are not rock type dependent, the existence and uniqueness as well as regularity of solutions to the PDEs have been studied. Given appropriate boundary and initial conditions and based on some assumptions on the data (see section below) one can determine the solution uniquely [4, 22, 23]. See also [18, 33] for the case of multiple rock types.

2.1. Boundary and initial conditions. Let us be given P_0, S_0 and P_D, S_D .

In the discussion below and in most experiments we use the following initial conditions

$$(11) \quad P(\mathbf{x}, 0) := \text{const} = P_0, \quad \mathbf{x} \in \Omega,$$

$$(12) \quad S(\mathbf{x}, 0) := \text{const} = S_0, \quad \mathbf{x} \in \Omega.$$

These conditions combined with (5) give initial values for the nonwetting phase pressure and saturation. Note that in the case (1) without gravity, a constant initial pressure and saturation represent an equilibrium solution. This is not true in case (2) with significant gravity where these initial conditions do not represent an equilibrium state. Finally, when considering multiple rock types in Example 3, we assume only (11) and an appropriately equivalent condition for the nonwetting phase, while $S(\mathbf{x}, 0)$ is determined from equality of capillary pressures.

The boundary $\partial\Omega$ consists of the no-flow part $\partial\Omega_N$ on which Neumann no-flow conditions are specified

$$(13) \quad \mathbf{u}_w \cdot \boldsymbol{\eta} = 0, \quad \mathbf{x} \in \partial\Omega_N, \quad t > 0,$$

$$(14) \quad \mathbf{u}_n \cdot \boldsymbol{\eta} = 0, \quad \mathbf{x} \in \partial\Omega_N, \quad t > 0$$

as well as of its complement $\partial\Omega_D$ in $\partial\Omega$, the part on which we impose Dirichlet boundary conditions

$$(15) \quad P(\mathbf{x}, t) = P_D, \quad \mathbf{x} \in \partial\Omega_D,$$

$$(16) \quad S(\mathbf{x}, t) = S_D, \quad \mathbf{x} \in \partial\Omega_D.$$

In most experiments on part of $\partial\Omega_D$ we impose $P_D \equiv P_0$ and/or $S_D \equiv S_0$.

2.2. Richards' equation. Richards' equation can be derived from (3), (4), (5), (6) by assuming that the nonwetting phase, hereby presumed to be air, remains at a constant pressure equal to the atmospheric pressure which for convenience one can set (in certain units) to 0

$$(17) \quad P_n \equiv 0.$$

Thereby one of the equations and variables is eliminated and one rewrites the equation (3) as follows

$$(18) \quad \phi \frac{\partial S}{\partial t} - \nabla \cdot \left(\frac{1}{\mu} \mathbf{K} k_w(\mathbf{x}, S) (\nabla P - \rho_w G \nabla D) \right) = 0,$$

where S, P are coupled via (5) and (17) as

$$(19) \quad P = -P_c(\mathbf{x}, S).$$

If $P_c(\cdot)$ is a smooth invertible function, then one can simply seek a solution in either variable. However, in general, $P_c(\cdot)$ exhibits strong degenerate behavior so that $\lim_{S \rightarrow 0} P_c(S) = \infty$. In addition, in some range of S and for some rock types, $P'_c(S) \approx 0$. Therefore depending on the particular rock type and on specific issues with behavior of $P_c(\mathbf{x}, S)$, there are advantages in using either P or S as the primary unknown.

In hydrology applications [57, 50] yet another version of (18) is preferred. Here the (convective, first order) gravity term is separated from the diffusive second order term, the nonlinearities are lumped together, and it is assumed that $\mathbf{K} \equiv K\mathbf{I}$ and that the rock-fluid properties are not rock-dependent. Finally the chain rule is applied to set

$$(20) \quad \mathbf{D}(S) := -\frac{1}{\mu} \mathbf{K} k_w(S) P'_c(S),$$

$$(21) \quad \mathbf{C}(S) := \frac{1}{\mu} \mathbf{K} k_w(S) \rho_w G \nabla(-D(\mathbf{x})),$$

from which (18) can be rewritten as a convection diffusion equation solved for S

$$(22) \quad \phi \frac{\partial S}{\partial t} + \nabla \cdot (\mathbf{D}(S) \nabla S) = \nabla \cdot (\mathbf{C}(S)).$$

Here the *diffusivity* coefficient $\mathbf{D}(S)$ is nonnegative definite and degenerate and the advective term $\mathbf{C}(S)$ is monotone nonincreasing degenerate. In case (1) the advective term vanishes $\mathbf{C}(S) \equiv \mathbf{0}$ and the equation has a nonlinear degenerate parabolic character. In case (2) the problem has nontrivial advection which, depending on the magnitude of capillary pressure, may or may not dominate the character of the flow.

The equation (22) can be also reformulated in terms of other variables: in hydrology it is popular to use the water content $\Theta := \phi S$ and pressure head $h := \frac{P}{G\rho_w}$ [50, 57].

Yet another formulation and change of variable are used in derivation of existence, uniqueness, and regularity theory for Richards' equation. One identifies a smooth variable, say u , by a Kirchoff transformation for which the well-posedness

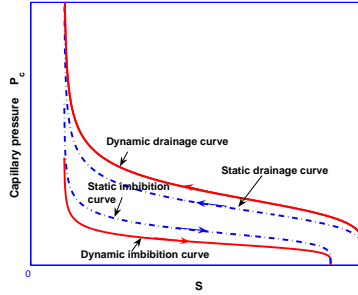


FIGURE 2. Idea of dynamic capillary pressure.

is studied; see [9, 36]. Then the values of S and/or P can be derived from u by means of a more or less degenerate transformation.

While the use of an auxiliary variable u is very helpful in understanding the transformed problem, it may or may not have a practical impact on applications in which the actual values of S and P need to be found. A similar remark applies to numerical methods applied to Richards' equation whose convergence for the transformed variable may be optimal in u albeit will exhibit sub-optimal convergence rates when studied in S, P .

2.2.1. Boundary and initial conditions. The boundary and initial conditions for Richards' equation follow from those for the two-phase flow (11), (12), (15), (13), (14), (16) noticing that by (17) the condition (14) is automatically satisfied and that (19) must be satisfied for all other conditions.

2.3. Dynamic capillary pressure. As mentioned above, the idea of incorporating dynamic effects in the capillary pressure-saturation relationship is to replace $P_c(\mathbf{x}, S)$ by $P_c(\mathbf{x}, S, \frac{\partial S}{\partial t})$ to account for dependence on time scale of getting to capillary equilibrium. Two main directions of models include the Hassanizadeh-model [42] and the Barenblatt-model [12, 11]. See Figure 2 for illustration. Also see a combination of play-type hysteresis and dynamic capillary pressure models in [13, 14].

In this paper we focus on the Hassanizadeh model and extend it to multiple rock types thereby assuming that (5) is replaced by (23)

$$(23) \quad P_c(\mathbf{x}, S, \frac{\partial S}{\partial t}) := P_c(\mathbf{x}, S) - \tau \frac{\partial S}{\partial t},$$

where $\tau \geq 0$ is a constant or it varies with \mathbf{x}, t .

Note that plugging this relationship to (19) we obtain, instead of (18),

$$(24) \quad \phi \frac{\partial S}{\partial t} + \nabla \cdot \left(\frac{\mathbf{K}k_w(S)}{\mu} \nabla P_c(S, \frac{\partial S}{\partial t}) \right) = \nabla \cdot \left(\frac{\mathbf{K}k_w(S)}{\mu} \rho_w G \nabla D(x) \right)$$

which can be rewritten in a generic nonlinear pseudo-parabolic form similar to (22)

$$(25) \quad \frac{\partial S}{\partial t} - \nabla \cdot (\mathbf{D}(S) \nabla S) = \nabla \cdot \mathbf{C}(S) + \nabla \cdot \left(\frac{Kk_w(S)}{\mu} \nabla \tau \frac{\partial S}{\partial t} \right).$$

2.4. Modeling flow in heterogeneous media. Consider now a full two-phase flow model with different rock types in a cell with coarse and fine sand described by $\mathbf{x} \in \Omega^I, \mathbf{x} \in \Omega^{II}$, respectively, in which fast and slow flow occur. In our experiments reported in Section 4.3 the parameters K^I and K^{II} differ by a factor of 10^3 . See Figure 3 for a schematic representation of the cell.

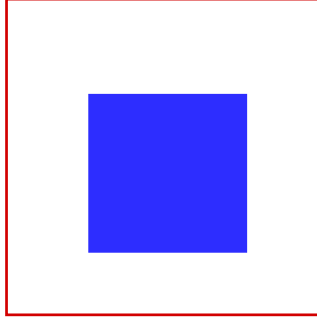


FIGURE 3. Schematic representation of a cell with two different media types: Ω^I (outside region) and Ω^{II} (inside).

It is well known [43] that in addition to variation in \mathbf{K} , one has to take into account rock-type dependent capillary-pressure properties

$$P_c(\mathbf{x}, S) = \begin{cases} P_c^I(S), & \mathbf{x} \in \Omega^I \\ P_c^{II}(S), & \mathbf{x} \in \Omega^{II} \end{cases}$$

as well as relative permeabilities k_w, k_n . In the dynamic capillary pressure model, we additionally have to take into account

$$\tau(\mathbf{x}) = \begin{cases} \tau^I, & \mathbf{x} \in \Omega^I \\ \tau^{II}, & \mathbf{x} \in \Omega^{II} \end{cases} .$$

3. Numerical approximation

Now we formulate two classes of numerical methods and their variants as applied to the two-phase problem system (3)–(6) and the Richards’ equation in the form (18) or (22). These two methods are the cell-centered Finite Difference method (FD), and the Locally Conservative Eulerian-Lagrangian Method (LCELM). A subset of these methods handle multiple rock types; all algorithms handle dynamic capillary pressure terms directly; that is, via (23).

We refer to [56] for an analogy between mixed finite element spaces of lowest Raviart-Thomas order on rectangles and cell-centered FD methods for single-phase flow, and to [65] for a convergence analysis of FD for a linear elliptic problem. Theoretically, via equivalence to mixed finite elements, the cell-centered FD provide, for simple linear problems, convergence order in primary unknowns (P, S) similar to the one in fluxes, or higher, via superconvergence. However, handling of nonlinear and degenerate terms and convection dominated problems requires extensions to expanded mixed methods [9, 69] and higher order temporal discretizations with the additional error due to the loss of consistency order, or to the stabilizing terms. We refer to [52] for a standard discretization of multiphase flow and to [53] for extensions of [56] to multiphase flow and treatment of boundary conditions, and to [40] for a discussion of stabilization procedures. Also, see [9, 36, 1, 15] for a variety of other schemes. Again, we do not attempt to give a complete set of references.

Method	Model	advective	diffusive	time discr.	unknown
R.LCELM	Richards (22)	-	a	use \bar{S}^n . See (40)	S
R.LCELM2	Richards (22)	-	a	use S^{n-1} . See (40)	S
R.FD1	Richards (22)	u	a	time-lagging	S
R.FD2	Richards (18)	u	u	time-lagging	S
R.FD3	Richards (18)	u	u	fully implicit	P
R.FD4	Richards (18)	u	u	time-lagging	P
R.FD5	Richards (18)	u	u	fully implicit	S
2PH	Two-phase	u	u	fully implicit (variable t.step)	P, S
2PH.E	Two-phase	u	u	time-lagging	P, S
2PH.F	Two-phase	u	u	fully implicit (fixed t.step)	P, S

TABLE 1. Numerical approximation schemes considered in this paper. Symbol u denotes upwinding, symbol a denotes arithmetic average.

In our work FD is applied to both the two-phase formulation and Richards' equation; we discuss for simplicity only the discretization for $d = 1$ but the results shown come from a general MATLAB implementation applicable to $d = 1, 2, 3$. The variants of FD presented here differ by the way we handle a) edge nonlinearities, and b) time-discretization and solving the resulting nonlinear system. Only the two-phase FD method is applied when rock types are different. When upwinding is applied, we expect the method to be at most $O(\Delta x + \Delta T)$ accurate, in either variant, with restrictions on the time step for the non-implicit variants due to the CFL condition. In the case i) with no gravity and away from degeneracy of P_c , and when diffusion terms are discretized using arithmetic averaging which gives higher order consistency, one could expect a convergence rate of $O((\Delta x)^2 + \Delta T)$.

It is well known that standard finite difference and finite element methods may inaccurately approximate convection-diffusion problems when the Péclet number is large. A variety of numerical methods have been developed to obtain better approximations; and many of these methods fall under the generic classification of Eulerian-Lagrangian methods [32, 34, 63, 29, 8]. Among them, a family of locally conservative Eulerian-Lagrangian methods (LCELM) was introduced [31] in the simulation of immiscible displacement in porous media; extensive computational experiments were presented in [31, 30, 3, 2]. Optimal-order error estimates have been derived for a finite difference analogue of LCELM for a semilinear parabolic equation in a single space variable [26] and for a multidimensional LCELM based on mixed finite elements for a semilinear parabolic equation [27].

Details on FD and LCELM discretization are provided in subsequent sections.

3.1. Finite difference approximations (FD). Consider first Richards' equation (18) and apply the FD method, fully implicit in time. Here for brevity we present the formulation for $d = 1$.

Discretize the spatial domain Ω as covered by a rectangular uniform grid of size Δx , with cell centers denoted by \mathbf{x}_i , and unknowns denoted by subscript i , $i = 1, \dots, nx$. The time variable is discretized by splitting $(0, T)$ into subintervals of variable size $\Delta T_n, n = 1, \dots, N$ where N is the number of time steps. Here the values of unknowns at time t^n are denoted by superscripts n .

We set

$$(26) \quad S_i^0 := S_0(\mathbf{x}_i), \quad i = 1, \dots, nx.$$

and then, for $n = 1, \dots, N$, we solve

$$\begin{aligned}
 (27) \quad & (\Delta x)^2 \phi(S_i^n - S_i^{n-1}) \\
 & - \Delta T_n K_{i+1/2} \frac{1}{\mu} k_{w,i+1/2}^* (P_{i+1}^n - P_i^n) \\
 & + \Delta T_n K_{i+1/2} \frac{1}{\mu} k_{w,i+1/2}^{**} \rho G (D_{i+1} - D_i) \\
 & + \Delta T_n K_{i-1/2} \frac{1}{\mu} k_{w,i-1/2}^* (P_i^n - P_{i-1}^n) \\
 & - \Delta T_n K_{i-1/2} \frac{1}{\mu} k_{w,i-1/2}^{**} \rho G (D_i - D_{i-1}) = 0, \quad i = 1, \dots, nx.
 \end{aligned}$$

In this scheme the main gist and the source of variants in formulations is in a) the choice of time-lagged coefficients or fully implicit solution, b) the handling of the advective $k_{w,i\pm 1/2}^{**}$ and the diffusive $k_{w,i\pm 1/2}^*$ edge nonlinearities, and finally c) the choice of primary unknowns: P or S . The various variants are summarized in Table 1 with details given as follows. Our methods resemble most closely those in [40, 69, 45, 53]. Boundary conditions are treated as in [53].

These variants follow standard textbook procedures [52, 43] but their choices may be delicate especially in the forthcoming context of dynamic capillary pressure terms; we give details for completeness.

For a) time discretization we use time-lagging whereby we set $n^* := n - 1$ or a fully implicit solution in which we use $n^* := n$. These definitions are used in computing coefficients of the (non)linear system.

In b) the choices include upwinding denoted in Table 1 by 'u' or arithmetic averages denoted by 'a'. Specifically, in upwinding, we set $k_{w,i+1/2}^* = k_w(S_i^{n^*})$ provided the potential difference $\Delta \psi_{i+1/2}^{n^*} := P_{i+1}^{n^*} - P_i^{n^*} - \rho G (D_{i+1} - D_i)$ is negative indicating that the flow is from the left. If the potential difference indicates flow from the right, we use the value $k_{w,i+1/2}^* = k_w(S_{i+1}^{n^*})$. In arithmetic averaging, we select $k_{w,i+1/2}^* = \frac{1}{2}(k_w(S_i^{n^*}) + k_w(S_{i+1}^{n^*}))$. Handling of $k_{w,i+1/2}^{**}$ and all other terms is analogous. The upwinding, albeit associated with lower convergence rate, provides additional stability and is applicable to more general models with compressibility and multiple rock types; see discussion in [40].

As concerns c), in the model (22) preferred by hydrologists and solved for S only, the term $\mathbf{D}(S)$ given by (20) is discretized using arithmetic averaging on the *entire* term and the term $\mathbf{C}(S)$ is discretized using upwinding as in all other FD variants. It appears that the averaging of the lumped form of $\mathbf{D}(S)$ leads to faster convergence than without the chain rule.

In the original model (18), when it is solved for P , the values of S and consequently the nonlinear properties are obtained via (19). Depending on the choice of time-lagging or fully implicit solution, the relation (19) is applied at the same time step or with time lagging.

Each of these choices has associated existing numerical theory which applies as long as the values of $k_w(\mathbf{x}, S)$, $P_c'(S)$ (or $\mathbf{D}(S)$) remain bounded away from singularities. In particular, it is known that for large advection, the use of arithmetic averaging in $k_{w,i+1/2}^{**}$ leads to instabilities. On the other hand, the use of upwinding increases numerical diffusion and leads to schemes that are slightly less accurate, at least away from degenerate conditions [48].

3.1.1. Discretization of two-phase model (3)–(4). In analogy to what was done for Richards' equation; that is, (3), one can write the discrete analogue for the nonwetting phase (4) and consider multiple variants of discretizations. For simplicity, here we report only on those discretization variants in which we use upwinding for both convective and diffusive terms. Time discretization can be implicit or time-lagged, the unknowns chosen are P, S .

3.1.2. Incorporating dynamic capillary pressure. In order to model dynamic capillary pressure, we discretize (23) as follows:

$$(28) \quad P_n^{n*} - P^{n*} = P_c(\mathbf{x}, S^{n*}) - \tau \frac{S^n - S^{n-1}}{\Delta T_n},$$

where for implicit solution we use $n^* = n$ and for time-lagging we use $n^* = n - 1$.

In the case of Richards' equation we use $P_n^{n*} \equiv 0$ from which follows a modification of (28).

3.1.3. Solution of (27). The system of discrete equations (27) for the time-lagged case when $n^* \equiv n - 1$ requires application of a linear solver. We use a direct solver from MATLAB suite for sparse matrices or an SOR iteration in which we iterate to very small tolerance.

In the fully implicit case when $n^* \equiv n$ we have a nonlinear system to solve at every time step. This is done by Newton's iteration with the Jacobian computed analytically and with the initial guess extrapolated from previous time steps. The time step is either fixed or it is controlled automatically depending on the success or failure of the Newton iteration. We refer to [46] for a general reference to solving nonlinear systems with Newton's method and to [44, 25, 45] for the work applicable to unsaturated flow.

3.2. Locally conservative Eulerian-Lagrangian method. LCELM is based on an operator-splitting procedure that separates the transport (convection) from the diffusion in (24) as follows:

1° **Initialize:**

$$(29) \quad S^0(\mathbf{x}) = S(\mathbf{x}, 0).$$

2° **Transport(Gravity):** For $n \geq 1$,

$$(30a) \quad \frac{\partial(\phi\bar{S})}{\partial t} + \nabla \cdot \left(\frac{\rho_w G}{\mu} \mathbf{K} k_w(\bar{S}) \nabla D \right) = 0, \quad t^{n-1} < t < t^n,$$

$$(30b) \quad \bar{S}(\mathbf{x}, t^{n-1}) = S^{n-1}(\mathbf{x}).$$

3° **Diffusion(Capillary pressure):** For $n \geq 1$,

$$(31a) \quad \frac{\partial(\phi\hat{S})}{\partial t} + \nabla \cdot \left(\frac{1}{\mu} \mathbf{K} k_w(\hat{S}) \left(P'_c(\hat{S}) \nabla \hat{S} - \nabla \tau \frac{\partial \hat{S}}{\partial t} \right) \right) = 0, \quad t^{n-1} < t < t^n,$$

$$(31b) \quad \hat{S}(\mathbf{x}, t^{n-1}) = \bar{S}(\mathbf{x}, t^n).$$

4° **Set**

$$(32) \quad S^n(\mathbf{x}) = \hat{S}(\mathbf{x}, t^n),$$

and go to 2°.

3.2.1. The local conservation relation. Let $M_{ij}, i = 1, \dots, nx, j = 1, \dots, ny$ be the $\Delta x \times \Delta y$ rectangle given by

$$M_{ij} = [\mathbf{x}_{i-1/2, j-1/2}, \mathbf{x}_{i+1/2, j-1/2}] \times [\mathbf{x}_{i-1/2, j-1/2}, \mathbf{x}_{i-1/2, j+1/2}].$$

Now, let us define a predecessor set for M_{ij} . Let $\mathbf{y}(t; \mathbf{x})$ be the solution of the final value problem given by

$$(33a) \quad \mathbf{y}' = \frac{\rho_w G \mathbf{K} k_w(S) \nabla D}{\mu \phi S},$$

$$(33b) \quad \mathbf{y}(t^n, \mathbf{x}) = \mathbf{x}.$$

Then, let

$$(34) \quad \partial \tilde{M}_{ij}^n = \{\mathbf{y}(t^{n-1}; \mathbf{x}) : \mathbf{x} \in \partial M_{ij}\},$$

and define the interior of $\partial \tilde{M}_{ij}^n$ to be the predecessor set \tilde{M}_{ij} at time t^{n-1} corresponding to M_{ij} at time t^n . Define the tube E_{ij}^n to be the set interior to M_{ij}, \tilde{M}_{ij}^n and the lateral boundary F_{ij}^n defined by the integral curve $\mathbf{y}(t; \mathbf{x}), t^{n-1} < t < t^n, \mathbf{x} \in \partial M_{ij}$. Then, the solution of (24) satisfies the relation

$$(35) \quad \int_{M_{ij}} \phi S^n d\mathbf{x} - \int_{\tilde{M}_{ij}} \phi S^{n-1} d\mathbf{x} + \int_{E_{ij}^n} \nabla \cdot \left(\frac{1}{\mu} \mathbf{K} k_w(\mathbf{x}, S) \left(P'_c(S) \nabla S - \nabla \tau \frac{\partial S}{\partial t} \right) \right) d\mathbf{x} dt = 0.$$

3.2.2. The approximate transport. The sets \tilde{M}_{ij}^n and E_{ij}^n depend explicitly on the solution S of (22), thus, they must be approximated using the values of the approximate solution, which will be denoted by $S^n, n = 0, 1 \dots N$. In this paper, we shall limit ourselves to the lowest order version of the LCELM based on a finite difference method in that S^n is taken to be piecewise constant. Note that S^n is multivalued on ∂M_{ij} , consequently, we will introduce a piecewise bilinear interpolation operator I as follows:

$$(36) \quad IS(\mathbf{x}_{i-1/2, j-1/2}) = (S_{i-1, j-1} + S_{i, j-1})/2,$$

i.e., IS is the upstream average. Now, assume that S^{n-1} is known. Denote the vertices of M_{ij} by $\mathbf{x}_{ij, k}, k = 1, \dots, 4$. Then, define an approximate predecessor \hat{Q}_{ij}^n as the quadrilateral having vertices

$$(37) \quad \hat{\mathbf{x}}_{ij, k}^n = \mathbf{x}_{ij, k} - \frac{\rho_w G \mathbf{K} k_w(IS(\mathbf{x}_{ij, k})) \nabla D(\mathbf{x}_{ij, k})}{\mu \phi IS(\mathbf{x}_{ij, k})} \Delta T, \quad k = 1, \dots, 4.$$

Let \hat{E}_{ij}^n be the tube formed with top M_{ij} and bottom \hat{Q}_{ij}^n . Then, the approximate local conservation equation can be written as

$$(38) \quad \int_{M_{ij}} \bar{S}^n d\mathbf{x} = \int_{\hat{Q}_{ij}^n} S^{n-1} d\mathbf{x}.$$

3.2.3. The diffusive fractional step. We shall approximate the solution of the diffusive fractional step (31) by one of two variants of time-lagged cell-centered finite difference methods, referred to below by R.LCELM and R.LCELM2. Here,

we for simplicity assume that τ is a constant and define:

$$\begin{aligned}
(39) \quad & (\Delta x)^2 (\Delta y)^2 \phi(S_{i,j}^n - \bar{S}_{i,j}^n) \\
& + \frac{(\Delta y)^2}{\mu} \mathbf{K}_{i+1/2,j} \left\{ \Delta T (k_w P'_c)^{*,n}_{i+1/2,j} (S_{i+1,j}^n - S_{i,j}^n) \right. \\
& \quad \left. - \tau k_{w,i+1/2,j}^{*,n} \left((S_{i+1,j}^n - S_{i,j}^n) - (\tilde{S}_{i+1,j}^n - \tilde{S}_{i,j}^n) \right) \right\} \\
& - \frac{(\Delta y)^2}{\mu} \mathbf{K}_{i-1/2,j} \left\{ \Delta T (k_w P'_c)^{*,n}_{i-1/2,j} (S_{i,j}^n - S_{i-1,j}^n) \right. \\
& \quad \left. - \tau k_{w,i-1/2,j}^{*,n} \left((S_{i,j}^n - S_{i-1,j}^n) - (\tilde{S}_{i,j}^n - \tilde{S}_{i-1,j}^n) \right) \right\} \\
& + \frac{(\Delta x)^2}{\mu} \mathbf{K}_{i,j+1/2} \left\{ \Delta T (k_w P'_c)^{*,n}_{i,j+1/2} (S_{i,j+1}^n - S_{i,j}^n) \right. \\
& \quad \left. - \tau k_{w,i,j+1/2}^{*,n} \left((S_{i,j+1}^n - S_{i,j}^n) - (\tilde{S}_{i,j+1}^n - \tilde{S}_{i,j}^n) \right) \right\} \\
& - \frac{(\Delta x)^2}{\mu} \mathbf{K}_{i,j-1/2} \left\{ \Delta T (k_w P'_c)^{*,n}_{i,j-1/2} (S_{i,j}^n - S_{i,j-1}^n) \right. \\
& \quad \left. - \tau k_{w,i,j-1/2}^{*,n} \left((S_{i,j}^n - S_{i,j-1}^n) - (\tilde{S}_{i,j}^n - \tilde{S}_{i,j-1}^n) \right) \right\} \\
& = 0,
\end{aligned}$$

where $(k_w P'_c)^{*,n}_{i\pm 1/2,j}$ and $k_{w,i\pm 1/2,j}^{*,n}$ are the arithmetic mean,

$$(k_w P'_c)^{*,n}_{i\pm 1/2,j} = \left((k_w P'_c)(\bar{S}_{i,j}^n) + (k_w P'_c)(\bar{S}_{i\pm 1,j}^n) \right) / 2$$

and

$$k_{w,i\pm 1/2,j}^{*,n} = \left(k_w(\bar{S}_{i,j}^n) + k_w(\bar{S}_{i\pm 1,j}^n) \right) / 2,$$

respectively and $(k_w P'_c)^{*,n}_{i,j\pm 1/2}$ and $k_{w,i,j\pm 1/2}^{*,n}$ are defined analogously. Here,

$$(40) \quad \tilde{S}_{i,j}^n = \begin{cases} \bar{S}_{i,j}^n & \text{in R_LCELM,} \\ S_{i,j}^{n-1} & \text{in R_LCELM2.} \end{cases}$$

A convergence analysis for R_LCELM2 for a linear problem has been done and will be presented in a subsequent paper.

4. Results

Here we report on numerical results for the schemes presented above. First, we illustrate the convergence and stability discussion given above; this is done via Example 1 in which no dynamic capillary pressure is taken into account i.e. $\tau \equiv 0$. Next, in Example 2 we compare the solutions with and without dynamic capillary pressure and are concerned with convergence and stability of the schemes. In Example 3 we demonstrate the use of multiple rock types combined with dynamic capillary pressure using a two-phase formulation.

Examples 1 and 2 are essentially 1D even though they are run with 2D codes; example 3 is run essentially in 3D but it has 2D features only.

Our studies are comprehensive and include simulations across all listed cases and schemes. However, for brevity we present only the typical and/or most interesting cases.

4.1. Example 1: convergence studies for $\tau \equiv 0$. Our examples include i) horizontal (1) and ii) vertical (2) infiltration problem, with parameters shown in Table 4.1. Initial saturation S_0 is constant, infiltration proceeds from the left at S_D . This is a purely “static” case with $\tau = 0$. Its purpose is to demonstrate convergence of methods which are used in Example 2 to simulate dynamic capillary pressure phenomena.

The data S_0, S_D for two-phase flow model are chosen so that (17) is essentially satisfied. Note, however, that this won't happen for just any choice of values S_0, S_D . The data P_0, P_D are adjusted accordingly.

Overall, the simulation parameters in this Example are chosen to demonstrate robustness of the methods for the relatively hard case which is the infiltration of a wetting front into an initially very dry soil. The infiltration is due to a boundary condition on i) left and ii) top, respectively, in each case imposing a pressure gradient. The right (bottom) boundary conditions are the same as the initial condition.

Recall that i) means the problem has only nonlinear (degenerate) diffusion terms while in case ii) it has additional nonlinear convective terms. Consulting Table 4.1 and Figure 1 we see that the case of sand II (fine) with large capillary pressure is diffusive, with or without gravity terms, while the case of sand I (coarse) has a strong convective term when gravity is present. This is evident in the solutions shown in Figure 4 which shows convergence study for Richards' equation and two-phase formulations.

It is clear that all methods converge, albeit R_FD1 and R_LCELM appear to have a higher convergence rate. Due to the upwinding R_FD2–R_FD5 have lower convergence rates. Moreover, all schemes and both models, Richards and two-phase, agree very well qualitatively and in most cases quantitatively. It seems that the choice of time-lagging or implicit solution is not essential as is the choice of the time step, as long as the time step is refined along with spatial grid parameter (studies not shown). Finally, what is not visible on the picture due to its resolution, is the fact that both methods R_LCELM and R_FD1 as opposed to R_FD2–R_FD5 appear to converge to a solution from *opposite* sides. This fundamental difference must be caused by the use of arithmetic averaging to *all* of $\mathbf{D}(S)$ in the former methods as opposed to handling them directly via a dependent variable in the latter case. In fact, the R_FD1 method appears to be closely related to standard Galerkin finite element discretization via the lumped discretization/averaging whereas the R_FD2–R_FD5 relate closer to the mixed methods.

Next, the choice of primary unknown: P or S in Richards' formulation with implicit time stepping appears to suggest, perhaps not surprisingly, that the use of P (implicit S) allows for larger time steps and smoother convergence of Newton's iteration than the use of S which is less diffusive.

More examples and comparisons are given in Figure 5 where we show results for multiple numerical methods for a given discretization, with gravity. Here we see again that R_LCELM and R_FD1 are capable of producing sharper fronts than R_FD2–R_FD5. The case without gravity is not shown but it features all curves in essentially the same place for all schemes.

Finally, as concerns comparison between modeling unsaturated flow using Richards' or two-phase flow model, it appears that for those cases when $P_n \approx 0$, the differences between (almost) equivalent methods R_FD2–R_FD5 and 2PH* are negligible. Here and below, 2PH* represents all the variants of FD based on the two-phase model.

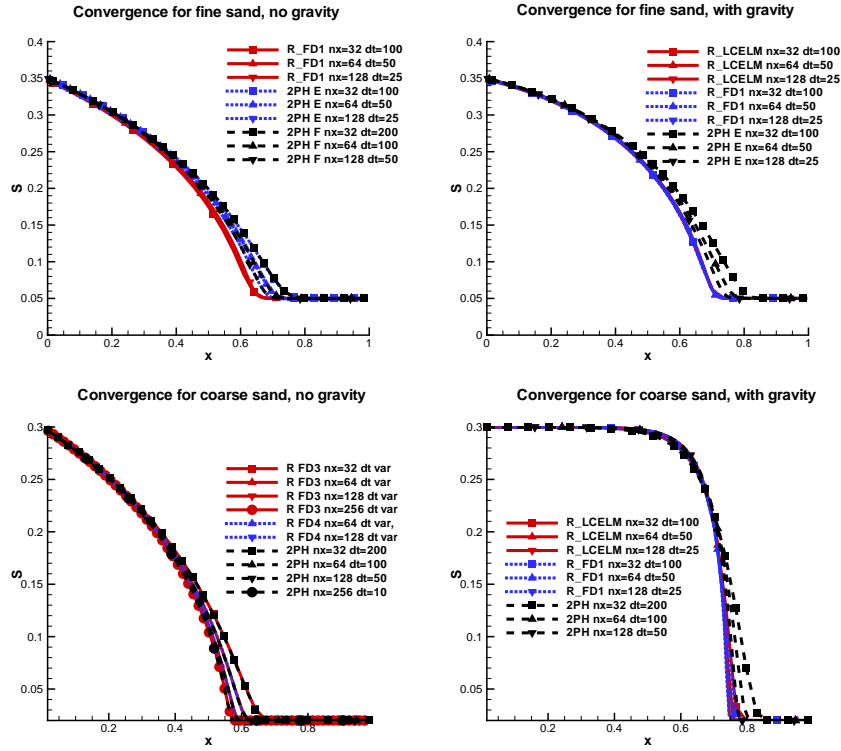


FIGURE 4. Convergence studies for fine sand II (top) and coarse sand I (bottom) examples, for different numerical methods; shown are cases with i) no convection (left, horizontal flow (1)) and ii) with convection (right, vertical flow (2)). Here nx varies from 32 to 256, and ΔT is changed appropriately.

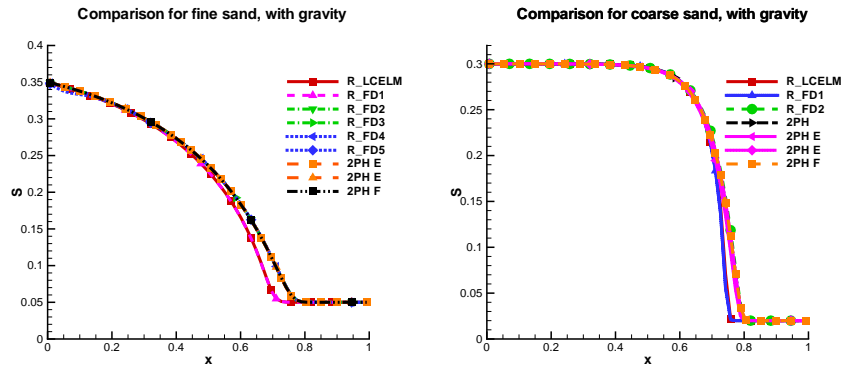


FIGURE 5. Comparison between numerical methods used for Richards' equation and two-phase flow formulation for both types of sand, with gravity.

4.2. Example 2: implementation of dynamic capillary pressure. Here we continue simulations with scenarios as in Example 1. However, now the dynamic

Physical properties of fluids:

$$\begin{aligned} \rho_w &= 10^3 [kg/m^3], \rho_n = 1.2 [kg/m^3], \\ \mu_w &= 10^{-3} [Pas], \mu_n = 1.78 \cdot 10^{-5} [Pas], \\ G &= 9.8066 [m/s^2]. \end{aligned}$$

Properties of porous medium:

$$\begin{aligned} \phi &= 0.4, \\ K^I &= 10^{-10} [m^2], \\ K^{II} &= 10^{-11} [m^2]. \end{aligned}$$

van Genuchten parameters:

$$\begin{aligned} \text{coarse sand I: } n &= 2.494, \alpha = 10^{-3}, \\ \text{fine sand II: } n &= 2.237, \alpha = 10^{-4}, \\ \text{all cases: } \epsilon &= 0.5, \gamma = 1/3. \end{aligned}$$

Boundary and initial conditions:

$$\begin{aligned} \text{coarse sand I: } S_0 &= 0.02, S_{left} = 0.30, \\ \text{fine sand II: } S_0 &= 0.05, S_{left} = 0.35. \end{aligned}$$

TABLE 2. Simulation parameters for Example 1 and Example 2, in SI units. The porous medium and rock-fluid properties are similar to those in the literature [43, 42]. We focus on effective saturations, therefore $S_{wr} = 0$.

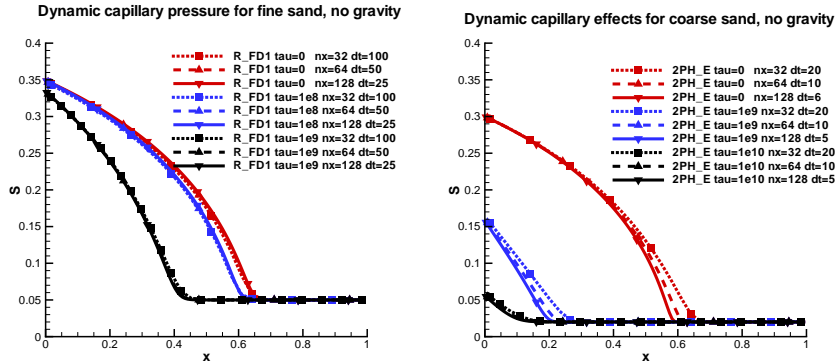


FIGURE 6. Influence of dynamic capillary pressure and convergence tests, no gravity; both fine and coarse sand cases.

capillary pressure terms are present, that is, $\tau > 0$. To a numerical analyst it actually comes as a surprise that in order to see the influence of dynamic capillary pressure, the values of τ (in the units used) have to be of several orders of magnitude, see however the identification of τ in [42].

Figures 6–9 present results of simulation for the case from Example 1, except with $\tau > 0$.

The first observation is that all methods (some cases are not shown) appear to converge and have smooth solutions; at least as long as no significant convection is present. We see again higher convergence rates for R.LCELM and R.FD1 and lower

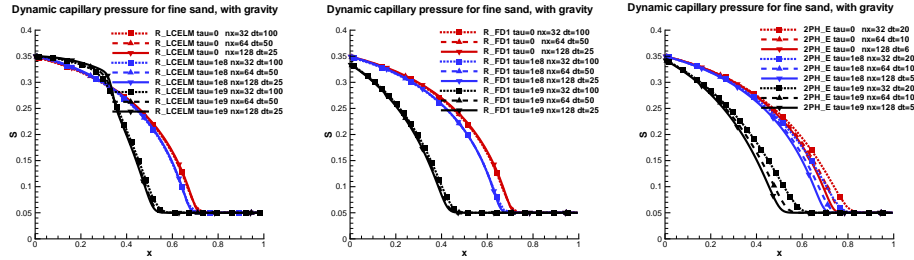


FIGURE 7. Convergence studies with dynamic capillary pressure: Fine sand with gravity (some convection, but not dominating). Solution profiles for R_LCELM2 are essentially identical with those for R_FD1 . Relative error, $\|R_FD1 - R_LCELM2\|_{\ell^\infty} / \|R_FD1\|_{\ell^\infty}$ is less than 0.16% for each τ when $nx = 128$, $dt = 25$.

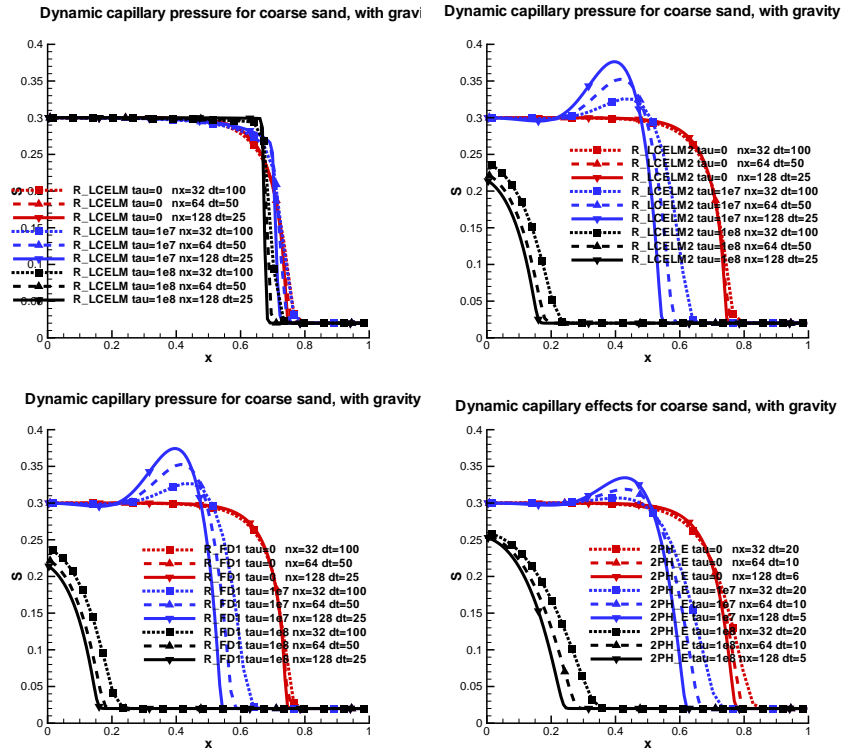


FIGURE 8. Convergence studies with dynamic capillary pressure. Coarse sand with gravity (very significant convection). Relative error, $\|R_FD1 - R_LCELM2\|_{\ell^\infty} / \|R_FD1\|_{\ell^\infty}$ is less than 6.8% for each τ when $nx = 128$, $dt = 25$.

for R_LCELM2 , R_FD2 – R_FD5 and $2PH^*$. This is consistent with the regularity theory presented in [59] which suggests that the presence of dynamic capillary pressure terms should not have de-stabilizing effects, at least in the purely parabolic case where convection is absent.

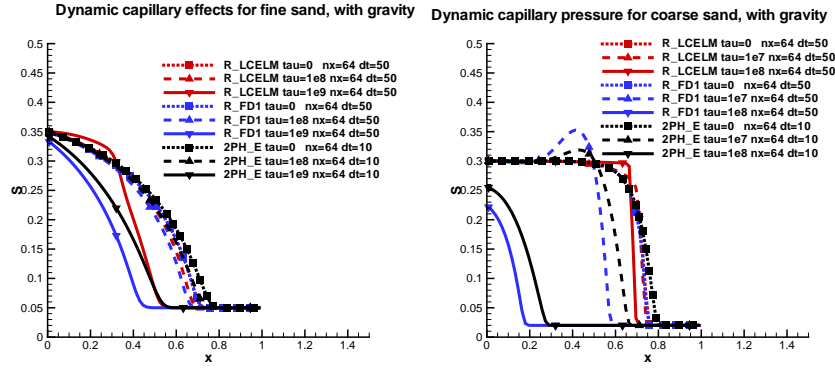


FIGURE 9. Comparison of results for dynamic capillary pressure. Both sand types with gravity, various methods.

Now, with some convection present (Figure 7), the convergence with the same observations is apparent. However, R.LCELM leads to a sharpening of the front, while R.LCELM2 doesn't. This can be explained by ability of LCELM to handle transport regardless of direction. The sharpening of the front visible in the R.LCELM case can be explained by the effect of terms with large τ which lead to a decrease of diffusion stronger for large S for this variant of time-stepping. See (40).

Then, for dominant convection (Figure 8), we obtain results which have non-monotone profiles for large τ for *all* FD-based methods, regardless of whether the Richards' or two-phase flow formulation is used. Note also that R.LCELM2 presents qualitatively the same profiles as FD-based methods. It is hard to assess convergence in this case as we do not have the true solution at this point. Also, we cannot speculate whether the apparent nonmonotonicity of profiles in Figure 8, present for all FD and R.LCELM2 solutions, relates to a numerical instability, or to a physical phenomenon. One could speculate that R.LCELM profiles are "real" and therefore instabilities in FD arise due to their lack of ability to approximate a sharp front which arises "against" the apparent convection direction. One could also bring back the discussion of nonmonotonicity in [40] for a vertical infiltration problem with heterogeneity.

To put these results in perspective, we recall that it has been reported in [42] that a straightforward discretization of the dynamic capillary pressure term leads to instabilities for large values of τ , albeit the details of the problematic and of improved formulation(s) were not given. On the other hand, the results reported in [51] focus on instabilities in the similarity solutions due to dynamic capillary pressure terms varying in t which are argued to be physical and not merely numerical phenomena.

Our results confirm that the straightforward inclusion of the dynamic capillary pressure does not lead to instabilities when convection terms are not present or are not dominant. At the same time, it is clear that the presence of advective terms which dominate diffusion may lead to physical appearance of various internal and boundary layers which may perhaps explain the nonmonotonicity of the solutions reported in Figure 8. At this point however we are not ready to make more general conclusions without further analysis which is outside the scope of this paper.

We close this discussion with remarks on time stepping and choice of primary unknowns. For all FD cases, the presence of dynamic terms appears to slow down the dynamics of the flow, similarly as reported in [42]. From a numerical point of view, this results in smoother performance of implicit methods, and very large time steps can be taken without harming the convergence of the Newton iteration. For example, the automatic time-stepping, if unrestricted, would allow the time step to grow by three orders of magnitude. However, the use of S as primary unknown in implicit formulations of Richards' equation required very small time steps as the Newton iteration was very sensitive to the domain of validity of (23).

The qualitative behavior of solutions for increasing τ comes without surprise. As shown in Figure 2, the larger dynamic terms during imbibition decrease the apparent diffusion due to capillary pressure, hence they should slow down the front which is moving partly due to nonlinear diffusion, and partly to convection. Where the two effects (diffusion and convection) become comparable, it is perhaps their competition that leads to instabilities which cannot be reliably captured with the numerical methods discussed here.

4.3. Example 3: dynamic capillary pressure and different rock types. In this experiment we show results of simulation for a 20×20 cell with $D(\mathbf{x}) = 0$ of heterogeneous medium such as shown in Figure 3. We are interested in the combined effects of heterogeneity and dynamic capillary pressure. The numerical scheme we choose is the implicit implementation of two-phase model with upwinding and variable time-stepping listed as 2PH in Table 1.

The data used for this example is very simple and except for the special data described below it is as in Table 4.1. Heterogeneity is associated with the ratio of 3 orders of magnitude difference in permeabilities $\mathbf{K}^I = 10^3 \cdot \mathbf{K}^{II}$. We use $k_w(\mathbf{x}, S) = S^2$, $k_n(\mathbf{x}, S) = (1 - S)^2$ for both rock types. As concerns static and dynamic capillary pressure relationships, we consider four experiments. The first two are with static capillary pressure and read a) $P_c^I(S) \equiv P_c^{II}(S) = \frac{1}{10\sqrt{S}}$; $\tau_I = 0$; $\tau_{II} = 0$, b) $P_c^I(S) = \frac{1}{10\sqrt{S}}$; $P_c^{II}(S) = 0.5(1 - S)$; $\tau^I = 0$; $\tau^{II} = 0$. In next two experiments we vary dynamic capillary pressure coefficients c) $P_c^I(S) = \frac{1}{10\sqrt{S}}$; $P_c^{II}(S) = 0.5(1 - S)$; $\tau^I = 10$; $\tau^{II} = 0$, d) $P_c^I(S) = \frac{1}{10\sqrt{S}}$; $P_c^{II}(S) = 0.5(1 - S)$; $\tau^I = 0$; $\tau^{II} = 10$. That is, in general, we have

$$(41) \quad P_c^I(S) \neq P_c^{II}(S).$$

All examples start from an initial equilibrium in which we are given a constant equilibrium pressure in both phases (hence, no pressure gradient) across both rock types. Such an equilibrium implies equality of capillary pressures and, in the case of (41), this implies inequality of initial saturations; see the initial condition of S for cases b), c), and d) shown below. On right and left boundaries of the cell we apply a Dirichlet boundary condition for saturations and pressures and no-flow condition is used on remaining boundaries. Thereby we create an infiltration front moving from right to left and which results in appearance of some internal boundary layers close to the outlet boundary.

Results of simulations are shown in Figures 10 and 11. They show the importance of both heterogeneity and dynamic effects.

In particular, comparison in Figure 10 shows significance of (41) starting at initial time step and in what follows. Case a) shows an example of bypassed air (nonwetting phase) pockets inside of the cell where the wetting phase has not invaded.

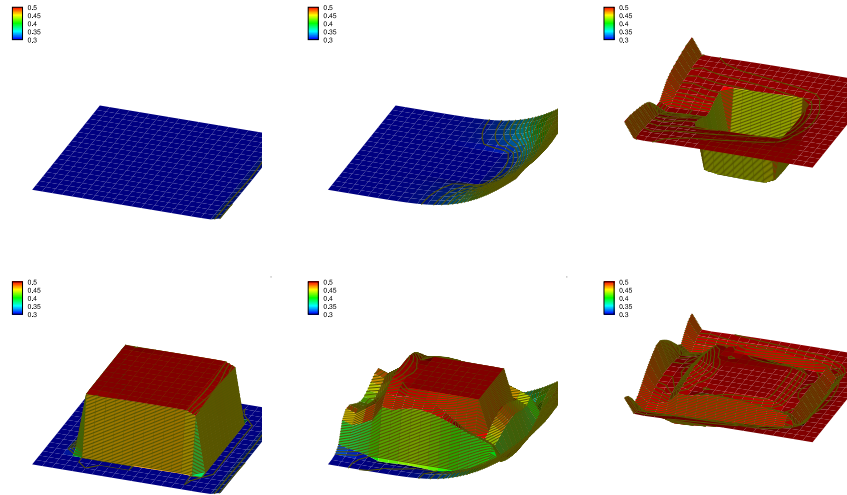


FIGURE 10. Results with static capillary pressure for cases a) (top) and b) (bottom), at the beginning, middle, and last time step of the simulation (from left to right).

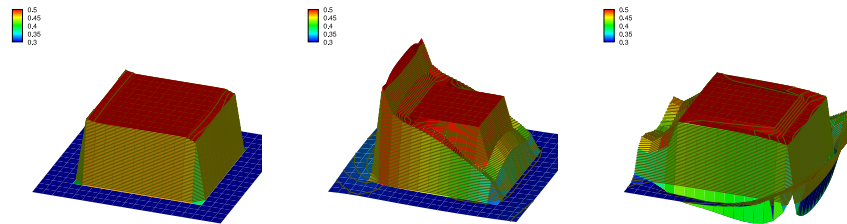


FIGURE 11. Initial time step (left) for cases c) and d) and results with dynamic capillary pressure at the end of simulation: case c) (middle) and d) (right).

Comparison of cases b) with dynamic cases of c) and (more physical) d) reveals that the delay effects in sand I (case c) slow down the flow in Ω^I surrounding Ω^{II} and lead to an internal boundary layer close to left boundary of Ω^{II} . The effect is reversed in case d). We mention here that it appears (Majid Hassanizadeh, private communications) that case d) is more physical: dynamic effects are likely to be more significant in fine sand where capillary pressure is more important than in coarse where they are not as important.

Characteristics of case d) will be the building blocks in our future construction of multiscale models of preferential flow with dynamic effects.

5. Conclusions

While the rigorous analysis for the nonlinear degenerate case is outside the scope of this paper, the convergence of FD formulation for (22) with dynamic capillary pressure (pseudo-parabolic) terms without convection i.e. $\mathbf{C}(S) \equiv 0$ has been confirmed by numerical experiments and is consistent with the findings of [35].

As reported above for case i) without gravity all the FD-based methods appear to converge and to have monotone solutions. For this case however the LCELM formulation is not relevant.

In the general case, we have shown above that in the presence of dynamic capillary pressure as well as different rock types, numerical solutions exhibit substantial differences with respect to those without dynamic terms. In cases without convection such as (22) with $\mathbf{C}(S) \equiv 0$, the solutions for large τ lag behind. This is consistent with the analysis in [60, 58] predicting that the size of jump in initial data, here due to the difference between initial and boundary conditions, decreases slowly when large τ in pseudo-parabolic terms is used.

However, it appears that the main difficulties and the presence of apparent instabilities are associated with the strong convective terms $\mathbf{C}(S)$ and large τ . In separate experiments not reported here we were able to determine, for each τ , the critical size of D_{fac} in $D(\mathbf{x}) = D_{fac}\mathbf{x}$ for which the method remains stable. In other words, there appears a critical Péclet number beyond which, due to the boundary or internal layers the numerical solution exhibits nonmonotonicities which remain stable with respect to the spatial and temporal grid refinement.

As concerns the convective term, our hope was that the use of LCELM would alleviate any potential instabilities. Indeed, the R_LCELM (but not R_LCELM2) results appear stable and have monotone behavior which is stable with respect to mesh refinement. While this approach offers different results than FD-based methods, we believe that more analysis of the time splitting and of the influence of convective terms is necessary before firm conclusions are drawn as to the nature and convergence of the methods.

Next, we believe that one needs a two-phase model rather than Richards' equation to properly model both the heterogeneities and dynamic capillary pressure effects. This follows from our observations on the size of nonwetting phase pressure P_n as monitored in the two-phase flow model which, albeit small compared to the value of P , exhibits substantial variations especially in dynamic case.

Finally, as seen from Example 3, the numerical methods for preferential flow should take into account both the variation rock type as well as proper models of accounting for dynamic effects such as dynamic capillary pressure. The impact of these two elements on the solutions is substantial, both qualitatively and quantitatively.

Acknowledgements

We would like to thank Majid Hassanizadeh for giving us the references to work [49] which pointed us also to other works in that volume, and for fruitful discussions. Most of our research was done before we became aware of these additional references. We thank Ralph Showalter and John Selker for discussions and references, and inspiration.

The research of the first author was partially supported by the grants NSF grant 0511190 and DOE grant 98089; the second author was partially supported by DOE grant 98089.

References

- [1] M. Afif and B. Amaziane. Convergence of finite volume schemes for a degenerate convection-diffusion equation arising in flow in porous media. *Comput. Methods Appl. Mech. Engrg.*, 191(46):5265–5286, 2002.

- [2] César Almeida, Jim Douglas, Jr., and Felipe Pereira. A new characteristics-based numerical method for miscible displacement in heterogeneous formations. *Comput. Appl. Math.*, 21(2):573–605, 2002. Special issue on multi-scale science (Nova Friburgo, 2000).
- [3] César Almeida, Jim Douglas, Jr., Felipe Pereira, Luis Carlos Roman, and Li-Ming Yeh. Algorithmic aspects of a locally conservative Eulerian-Lagrangian method for transport-dominated diffusive systems. In *Fluid flow and transport in porous media: mathematical and numerical treatment (South Hadley, MA, 2001)*, volume 295 of *Contemp. Math.*, pages 37–48. Amer. Math. Soc., Providence, RI, 2002.
- [4] H. W. Alt and E. di Benedetto. Nonsteady flow of water and oil through inhomogeneous porous media. *Ann. Scuola Norm. Sup. Pisa Cl. Sci. (4)*, 12(3):335–392, 1985.
- [5] H.W. Alt, S. Luckhaus, and A. Visintin. On nonstationary flow through porous media. *Ann. Mat. Pura Appl.*, 136(4):303–316, 1984.
- [6] T. Arbogast. The existence of weak solutions to single porosity and simple dual-porosity models of two-phase incompressible flow. *Nonlinear Analysis, Theory, Methods and Applications*, 19:1009–1031, 1992.
- [7] T. Arbogast, A. Chilakapati, and M. F. Wheeler. A characteristic-mixed method for contaminant transport and miscible displacement. In *Computational methods in water resources, IX, Vol. 1 (Denver, CO, 1992)*, pages 77–84. Comput. Mech., Southampton, 1992.
- [8] T. Arbogast and M. F. Wheeler. A characteristics-mixed finite element method for advection-dominated transport problems. *SIAM J. Numer. Anal.*, 32:404–424, 1995.
- [9] Todd Arbogast, Mary F. Wheeler, and Nai-Ying Zhang. A nonlinear mixed finite element method for a degenerate parabolic equation arising in flow in porous media. *SIAM J. Numer. Anal.*, 33(4):1669–1687, 1996.
- [10] Douglas N. Arnold, Jim Douglas, Jr., and Vidar Thomée. Superconvergence of a finite element approximation to the solution of a Sobolev equation in a single space variable. *Math. Comp.*, 36(153):53–63, 1981.
- [11] G. I. Barenblatt, D. B. Silin, and T. W. Patzek. The mathematical model of non-equilibrium effects in water-oil displacement. *SPEJ*, 8(4):409–416, December 2003.
- [12] G.I. Barenblatt and A. A. Gil'man. A mathematical model of non-equilibrium counter-current capillary imbibition. *J. Eng. Phys.*, 52(3):456–461, 1987.
- [13] A. Y. Beliaev and R. J. Schotting. Analysis of a new model for unsaturated flow in porous media including hysteresis and dynamic effects. *Comput. Geosci.*, 5(4):345–368 (2002), 2001.
- [14] A. Yu. Beliaev and S. M. Hassanizadeh. A theoretical model of hysteresis and dynamic effects in the capillary relation for two-phase flow in porous media. *Transp. Porous Media*, 43(3):487–510, 2001.
- [15] L. Bergamaschi and M. Putti. Mixed finite elements and Newton-type linearizations for the solution of Richards' equation. *Internat. J. Numer. Methods Engrg.*, 45(8):1025–1046, 1999.
- [16] Alain Bourgeat. Two-phase flow. In U. Hornung, editor, *Homogenization and porous media*, volume 6 of *Interdiscip. Appl. Math.*, pages 97–187. Springer, New York, 1997.
- [17] Alain Bourgeat and Abdelkader Hidani. Effective model of two-phase flow in a porous medium made of different rock types. *Appl. Anal.*, 58(1-2):1–29, 1995.
- [18] Alain Bourgeat and Abdelkader Hidani. A result of existence for a model of two-phase flow in a porous medium made of different rock types. *Appl. Anal.*, 56(3-4):381–399, 1995.
- [19] Alain Bourgeat and Mikhail Panfilov. Effective two-phase flow through highly heterogeneous porous media: capillary nonequilibrium effects. *Comput. Geosci.*, 2(3):191–215, 1998.
- [20] M. A. Celia, E. T. Bouloutas, and R. L. Zarba. A general mass-conservative numerical solution for the unsaturated flow equation. *Water Resour. Res.*, 26:1483–1496, 1990.
- [21] Z. Chen, R. E. Ewing, Q. Jiang, and A. M. Spagnuolo. Error analysis for characteristics-based methods for degenerate parabolic problems. *SIAM J. Numer. Anal.*, 40(4):1491–1515, 2002.
- [22] Zhangxin Chen. Degenerate two-phase incompressible flow. I. Existence, uniqueness and regularity of a weak solution. *J. Differential Equations*, 171(2):203–232, 2001.
- [23] Zhangxin Chen. Degenerate two-phase incompressible flow. II. Regularity, stability and stabilization. *J. Differential Equations*, 186(2):345–376, 2002.
- [24] R. E. Collins. *Flow of fluids through porous materials*. PennWell Books, Tulsa, Oklahoma, 1961.
- [25] C. N. Dawson, H. Klie, M. F. Wheeler, and C. Woodward. A parallel, implicit, cell-centered method for two-phase flow with a preconditioned Newton-Krylov solver. *Comput. Geosci.*, 1:215–249, 1997.
- [26] J. Douglas, Jr. and C.-S. Huang. The convergence of a locally conservative eulerian-lagrangian finite difference method for a semilinear parabolic equation. *BIT*, pages 980–989, 2001.

- [27] J. Douglas, Jr., A. M. Spagnuolo, and S.-Y. Yi. The convergence of a multidimensional locally conservative, Eulerian-Lagrangian finite element method for a semilinear parabolic equation. manuscript, 2007.
- [28] Jim Douglas, Jr. and T. Arbogast. Dual-porosity models for flow in naturally fractured reservoirs. In J. H. Cushman, editor, *Dynamics of Fluids in Hierarchical Porous Media*, pages 177–221. Academic Press, 1990.
- [29] Jim Douglas, Jr., Chieh-Sen Huang, and Felipe Pereira. The modified method of characteristics with adjusted advection. *Numer. Math.*, 83(3):353–369, 1999.
- [30] Jim Douglas, Jr., Felipe Pereira, and Li-Ming Yeh. A locally conservative Eulerian-Lagrangian method for flow in a porous medium of a mixture of two components having different densities. In *Numerical treatment of multiphase flows in porous media (Beijing, 1999)*, volume 552 of *Lecture Notes in Phys.*, pages 138–155. Springer, Berlin, 2000.
- [31] Jim Douglas, Jr., Felipe Pereira, and Li-Ming Yeh. A locally conservative Eulerian-Lagrangian numerical method and its application to nonlinear transport in porous media. *Comput. Geosci.*, 4(1):1–40, 2000.
- [32] J. Douglas, Jr. and T. F. Russell. Numerical methods for convection-dominated diffusion problems based on combining the method of characteristics with finite element or finite difference procedures. *SIAM J. Numer. Anal.*, 19:871–885, 1982.
- [33] C.J. Van Duijn, J. Molenaar, and M.J. De Neef. The effect of capillary forces on immiscible two-phase flow in heterogeneous porous media. *Trans. Porous Media*, 21:71–93, 1995.
- [34] R. E. Ewing, T. F. Russell, and M. F. Wheeler. Convergence analysis of an approximation of miscible displacement in porous media by mixed finite elements and a modified method of characteristics. *Comp. Meth. Appl. Mech. Eng.*, 47:73–92, 1984.
- [35] Richard E. Ewing. Numerical solution of Sobolev partial differential equations. *SIAM J. Numer. Anal.*, 12:345–363, 1975.
- [36] Robert Eymard, Michaël Gutnic, and Danielle Hilhorst. The finite volume method for Richards equation. *Comput. Geosci.*, 3(3-4):259–294 (2000), 1999.
- [37] William H. Ford. Galerkin approximations to non-linear pseudo-parabolic partial differential equations. *Aequationes Math.*, 14(3):271–291, 1976.
- [38] William H. Ford and T. W. Ting. Stability and convergence of difference approximations to pseudo-parabolic partial differential equations. *Math. Comp.*, 27:737–743, 1973.
- [39] William H. Ford and T. W. Ting. Uniform error estimates for difference approximations to nonlinear pseudo-parabolic partial differential equations. *SIAM J. Numer. Anal.*, 11:155–169, 1974.
- [40] P. A. Forsyth and M. C. Kropinski. Monotonicity considerations for saturated-unsaturated subsurface flow. *SIAM J. Sci. Comput.*, 18(5):1328–1354, 1997.
- [41] W.G. Gray and S.M. Hassanizadeh. Paradoxes and realities in unsaturated flow theory. *Water Resour. Res.*, 27:1847–1854, 1991.
- [42] S.M. Hassanizadeh, M.A. Celia, and H.K. Dahle. Dynamic effects in the capillary pressure-saturation relationship and their impacts on unsaturated flow. *Vadose Zone Journal*, 1:38–57, 2002.
- [43] R. Helmig. *Multiphase flow and transport processes in the Subsurface*. Springer, 1997.
- [44] E. W. Jenkins, C. T. Kelley, C. E. Kees, and C. T. Miller. An aggregation-based domain decomposition preconditioner for groundwater flow. *SIAM Journal on Scientific Computing*, 23(2):430–441, 2001.
- [45] Jim E. Jones and Carol S. Woodward. Newton-krylov-multigrid solvers for large-scale, highly heterogeneous, variably saturated flow problems. *Advances in Water Resources*, 24:763–774, 2001.
- [46] C. T. Kelley. *Iterative methods for linear and nonlinear equations*. SIAM, Philadelphia, 1995.
- [47] R.J. Lenhard, M. Oostrom, and M.D. White. Modeling fluid flow and transport in variably saturated porous media with the STOMP simulator. 2. Verification and validation exercises. *Advances in Water Resources*, 18(6), 1995.
- [48] Randall J. LeVeque. *Numerical methods for conservation laws*. Lectures in Mathematics ETH Zürich. Birkhäuser Verlag, Basel, 1990.
- [49] S. Mantney, S. M. Hassanizadeh, and R. Helmig. Macro-scale dynamic effects in homogeneous and heterogeneous porous media. *Transp. Porous Med.*, 58:121–145, 2005.
- [50] Ghislain De Marsily. *Quantitative Hydrogeology: Groundwater Hydrology for Engineers*. Academic Press, 1986.
- [51] J. L. Nieber, R. Z. Dautov, and A. G. Egorov. Dynamic capillary pressure mechanism for instability in gravity-driven flows: Review and extension to very dry conditions. In D. B.

- Das and S. M. Hassanizadeh, editors, *Upscaling Multiphase Flow in Porous Media*, pages 147–172. Springer, 2005.
- [52] D. W. Peaceman. *Fundamentals of numerical reservoir simulation*. Elsevier Scientific Publishing Company, Amsterdam-Oxford-New York, first edition, 1977.
- [53] M. Peszyńska, E. Jenkins, and M. F. Wheeler. Boundary conditions for fully implicit two-phase flow model. In Xiaobing Feng and Tim P. Schulze, editors, *Recent Advances in Numerical Methods for Partial Differential Equations and Applications*, volume 306 of *Contemporary Mathematics Series*, pages 85–106. American Mathematical Society, 2002.
- [54] Florin Radu, Iuliu Sorin Pop, and Peter Knabner. Order of convergence estimates for an Euler implicit, mixed finite element discretization of Richards' equation. *SIAM J. Numer. Anal.*, 42(4):1452–1478 (electronic), 2004.
- [55] T. Russell. Formulation of a model accounting for capillary non-equilibrium in naturally fractured subsurface formations. In R. E. Ewing and D. Copeland, editors, *Proceedings of the Fourth Wyoming Enhanced Oil Recovery Symposium*, pages 103–114, 1988.
- [56] T. F. Russell and M. F. Wheeler. Finite element and finite difference methods for continuous flows in porous media. In R. E. Ewing, editor, *The Mathematics of Reservoir Simulation*, pages 35–106. SIAM, Philadelphia, 1983.
- [57] J.S. Selker, C. K. Keller, and J. T. McCord. *Vadose Zone Processes*. Lewsi Publishers, 1999.
- [58] R. E. Showalter. Partial differential equations of Sobolev-Galpern type. *Pacific J. Math.*, 31:787–793, 1969.
- [59] R. E. Showalter. Local regularity, boundary values and maximum principles for pseudoparabolic equations. *Applicable Anal.*, 16(3):235–241, 1983.
- [60] R. E. Showalter and T. W. Ting. Pseudoparabolic partial differential equations. *SIAM J. Math. Anal.*, 1:1–26, 1970.
- [61] Tsuan Wu Ting. Parabolic and pseudo-parabolic partial differential equations. *J. Math. Soc. Japan*, 21:440–453, 1969.
- [62] J. Touma and M. Vauclin. Experimental and numerical analysis of two-phase infiltration in a partially saturated soil. *Transport in Porous Media*, pages 27–55, 1986.
- [63] Hong Wang, Richard E. Ewing, and Thomas F. Russell. Eulerian-Lagrangian localized adjoint methods for convection-diffusion equations and their convergence analysis. *IMA J. Numer. Anal.*, 15(3):405–459, 1995.
- [64] M. Weiler, T. Uchida, and J.J. McDonnell. Connectivity due to preferential flow controls water flow and solute transport at the hillslope scale. In D. Post, editor, *Proc. MODSIM 2003, Interactive modeling of Biophysical, Social and Biological Systems for Resource Management Solutions*, pages 398–403, 2003.
- [65] Alan Weiser and Mary Fanett Wheeler. On convergence of block-centered finite differences for elliptic problems. *SIAM J. Numer. Anal.*, 25(2):351–375, 1988.
- [66] D. Wildenschild, J. W. Hopmanns, and J. Simunek. Flow rate dependence of soil hydraulic characteristics. *Soil Sci. Soc. Am. J.*, 65:35–48, 2001.
- [67] D. Wildenschild, J.W. Hopmans, A.J.R. Kent, and M.L. Rivers. A quantitative study of flow-rate dependent processes using x-ray microtomography. 2004.
- [68] D. Wildenschild and K.H. Jensen. Laboratory investigations of effective flow behavior in unsaturated heterogeneous soils. *Water Res. Research*, 35(1):17–27, January 1999.
- [69] Carol S. Woodward and Clint N. Dawson. Analysis of expanded mixed finite element methods for a nonlinear parabolic equation modeling flow into variably saturated porous media. *SIAM J. Numer. Anal.*, 37(3):701–724 (electronic), 2000.

Department of Mathematics, Oregon State University, Corvallis, OR 97331
 E-mail: mpez@math.oregonstate.edu and yis@math.oregonstate.edu
 URL: <http://www.math.oregonstate.edu/~mpez/> and
 URL: <http://www.math.oregonstate.edu/people/view/yis>